

Spider silk reinforced by graphene or carbon nanotubes

This content has been downloaded from IOPscience. Please scroll down to see the full text.

2017 2D Mater. 4 031013

(<http://iopscience.iop.org/2053-1583/4/3/031013>)

View [the table of contents for this issue](#), or go to the [journal homepage](#) for more

Download details:

IP Address: 129.169.173.66

This content was downloaded on 22/08/2017 at 10:36

Please note that [terms and conditions apply](#).

You may also be interested in:

[Nanomechanics of silk: the fundamentals of a strong, tough and versatile material](#)

Isabelle Su and Markus J Buehler

[Introducing biomimetic shear and ion gradients to microfluidic spinning improves silk fiber strength](#)

David Li, Matthew M Jacobsen, Nae Gyune Rim et al.

[Cross-linking multiwall carbon nanotubes using PFPA to build robust, flexible and highly aligned large-scale sheets and yarns](#)

Yoku Inoue, Kazumichi Nakamura, Yuta Miyasaka et al.

[Spider-silk-like shape memory polymer fiber for vibration damping](#)

Qianxi Yang and Guoqiang Li

[Protein unfolding versus \$\beta\$ -sheet separation in spider silk nanocrystals](#)

Parvez Alam

[Biomimetic calcium phosphate coatings on recombinant spider silk fibres](#)

Liang Yang, My Hedhammar, Tobias Blom et al.

[Biological and mechanical evaluation of poly\(lactic-co-glycolic acid\)-based composites reinforced with 1D, 2D and 3D carbon biomaterials for bone tissue regeneration](#)

Tejinder Kaur, Senthilguru Kulanthaivel, Arunachalam Thirugnanam et al.

[Electromechanical behavior of carbon nanotube fibers under transverse compression](#)

Yuanyuan Li, Weibang Lu, Subramani Sockalingam et al.

2D Materials



LETTER

Spider silk reinforced by graphene or carbon nanotubes

RECEIVED
19 February 2017

REVISED
20 June 2017

ACCEPTED FOR PUBLICATION
30 June 2017

PUBLISHED
14 August 2017

Emiliano Lepore¹, Federico Bosia², Francesco Bonaccorso^{3,4}, Matteo Bruna³, Simone Taioli^{5,6}, Giovanni Garberoglio⁵, Andrea C Ferrari³ and Nicola Maria Pugno^{1,7,8}

¹ Laboratory of Bio-inspired & Graphene Nanomechanics, Department of Civil, Environmental and Mechanical Engineering, University of Trento, Via Mesiano 77, 38123 Trento, Italy

² Department of Physics and 'Nanostructured Interfaces and Surfaces' Centre, Università di Torino, Via P. Giuria 1, 10125, Torino, Italy

³ Cambridge Graphene Centre, University of Cambridge, 9 JJ Thomson Avenue, Cambridge, CB3 0FA, United Kingdom

⁴ Istituto Italiano di Tecnologia, Graphene Labs, Via Morego 30, 16163 Genova, Italy

⁵ European Centre for Theoretical Studies in Nuclear Physics and Related Areas, Bruno Kessler Foundation and Trento Institute for Fundamental Physics and Applications, Trento, Italy

⁶ Faculty of Mathematics and Physics, Charles University, Prague, Czechia

⁷ School of Engineering and Materials Science, Queen Mary University of London, Mile End Road, London E1 4NS, United Kingdom

⁸ Ket Lab, Edoardo Amaldi Foundation, Italian Space Agency, Via del Politecnico snc, 00133 Rome, Italy

E-mail: nicola.pugno@unitn.it

Keywords: graphene, spider silk, toughness, strength, carbon nanotubes

Supplementary material for this article is available [online](#)

Abstract

Spider silk has promising mechanical properties, since it conjugates high strength (~ 1.5 GPa) and toughness (~ 150 J g⁻¹). Here, we report the production of silk incorporating graphene and carbon nanotubes by spider spinning, after feeding spiders with the corresponding aqueous dispersions. We observe an increment of the mechanical properties with respect to pristine silk, up to a fracture strength ~ 5.4 GPa and a toughness modulus ~ 1570 J g⁻¹. This approach could be extended to other biological systems and lead to a new class of artificially modified biological, or 'bionic', materials.

Introduction

Silkworm silks have been widely used by mankind for millennia, but only recently their mechanical properties and structure have been investigated in depth [1, 2]. An increasing number of studies also focuses on spider silk, due to its promising mechanical (~ 10 GPa Young's modulus, ~ 1.5 GPa strength [3, 4], $\sim 100\%$ ultimate strain [5]) and thermal properties (~ 400 W m⁻¹ · K⁻¹ thermal conductivity [6]), combined with biocompatibility [7] and biodegradability [5, 7, 8]. This makes it potentially useful in practical applications, such as wear-resistant lightweight clothing [9], bullet-proof vests [10], ropes [11], nets [12], bandages [13], surgical threads [14], artificial tendons or ligaments [15], biodegradable food wraps [16], or rust-free panels on vehicles [17]. E.g., in [18], researchers used individual spider silk fibres braided together to create sutures for flexor tendon repair. Enhanced silk mechanical properties could further improve the fatigue strength and lifetime of these structures.

The production of silk is key to the spiders' evolutionary success and has been perfected over 400

million years [7]. Silk is generally described as a semi-crystalline [19], biocompatible [7], composite biopolymer [5], and comprises the amino acids alanine, glycine and serine, organized into semi-amorphous helical-elastic α -chains and β -pleated nanocrystals [20, 21]. From a mechanical point of view, it is considered amongst the best spun polymer fibres in terms of tensile strength [3, 4] and ultimate strain [5], therefore toughness [11], even when compared with the best performing synthetic fibres, such as Kevlar [22]. Silk spinning involves a number of biological, chemical and physical processes [23], leading to its superior mechanical properties.

The natural presence of biominerals in the protein matrix and hard tissues of insects [24], worms [25] and snails [26] enables high strength and hardness (>500 MPa) of teeth [27, 28], jaws [28, 29], and mandibles [30, 31]. Thus, the artificial incorporation of various nanomaterials in biological protein structures to obtain improved mechanical properties should, in principle, be possible. A number of groups introduced inorganic nanoparticles [32], semiconducting crystals [33] or carbon nanotubes (CNTs) [34] on the surface of spider silk fibres, achieving an

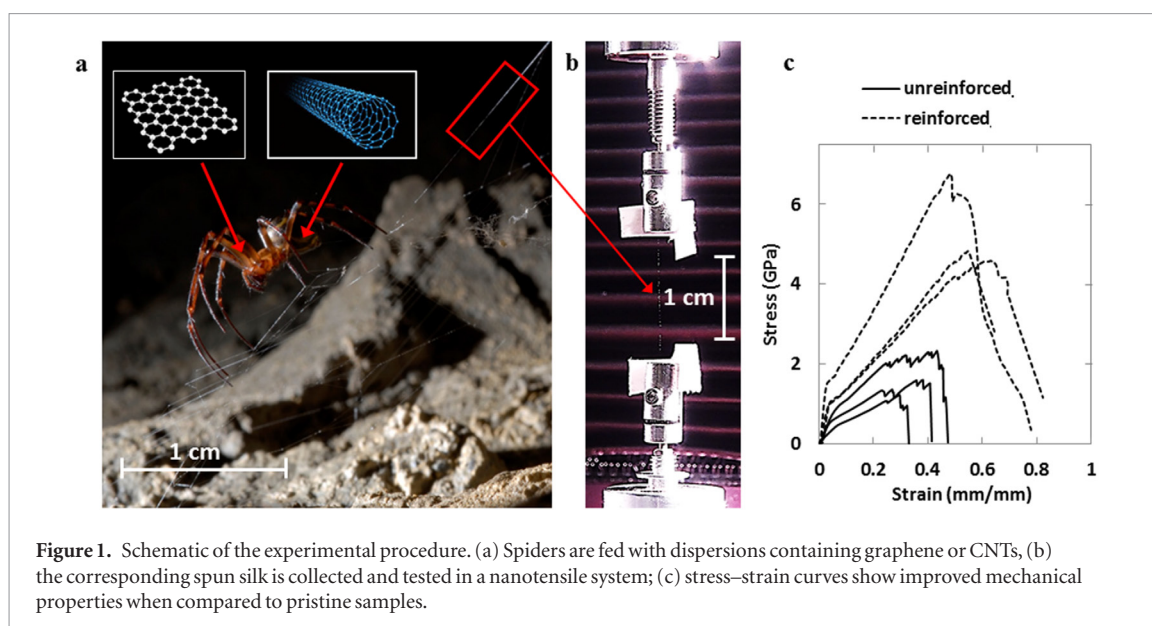


Table 1. Mechanical properties (average values) of RS samples.

Spider n.	Diameter (μm)	Number of threads	Young's modulus (GPa)	Ultimate strain (mm mm^{-1})	Fracture strength (MPa)	Toughness modulus (MPa)
1	0.51 ± 0.10	15	6.0 ± 3.6	0.29 ± 0.12	795.2 ± 500.1	128.2 ± 97.2
2	0.72 ± 0.15	7	27.3 ± 5.0	0.58 ± 0.23	2397.2 ± 635.5	713.0 ± 138.5
3	0.75 ± 0.11	10	13.4 ± 6.9	0.46 ± 0.40	1257.5 ± 1299.3	422.6 ± 567.6
4	0.69 ± 0.06	108	1.9 ± 0.6	1.38 ± 1.11	465.1 ± 119.0	235.6 ± 126.2
5	0.71 ± 0.06	128	3.2 ± 0.8	1.02 ± 0.30	534.7 ± 222.1	172.4 ± 77.4
6	0.72 ± 0.02	2	37.1 ± 19.6	0.28 ± 0.06	4045.9 ± 1391.6	732.1 ± 354.9
7	0.86 ± 0.07	10	15.1 ± 6.4	0.39 ± 0.07	1726.6 ± 565.3	476.4 ± 257.8
8	0.65 ± 0.05	113	2.1 ± 2.0	0.69 ± 0.40	179.7 ± 164.0	61.1 ± 79.3
9	0.51 ± 0.04	95	5.9 ± 5.0	0.53 ± 0.44	580.7 ± 482.9	205.3 ± 179.8
10	0.81 ± 0.09	48	3.0 ± 1.5	0.55 ± 0.08	281.2 ± 179.6	75.3 ± 45.8
11	0.51 ± 0.05	111	24.3 ± 13.5	0.75 ± 0.29	1969.1 ± 1158.8	764.7 ± 640.5
12	0.83 ± 0.06	17	3.1 ± 0.1	0.77 ± 0.10	173.4 ± 0.1	48.9 ± 0.1
13	0.66 ± 0.06	74	5.5 ± 5.0	0.88 ± 0.74	648.6 ± 501.9	320.3 ± 385.8
14	1.02 ± 0.03	64	3.8 ± 1.1	1.71 ± 0.87	364.0 ± 164.1	247.8 ± 111.2
15	0.54 ± 0.02	4	9.2 ± 1.5	0.26 ± 0.06	825.2 ± 182.9	101.8 ± 9.6

enhancement of toughness [35], or novel properties, such as magnetism [32] or electrical conductivity [34]. This type of reinforcement or functionalization could further make silk potentially attractive for a wide range of applications, from garment textiles [9] to sensing devices [34], from medical applications, such as suture threads [14] or tissue regeneration materials [15], to defence applications such as flak jackets [10], currently limited by the silk large deformability [36–39].

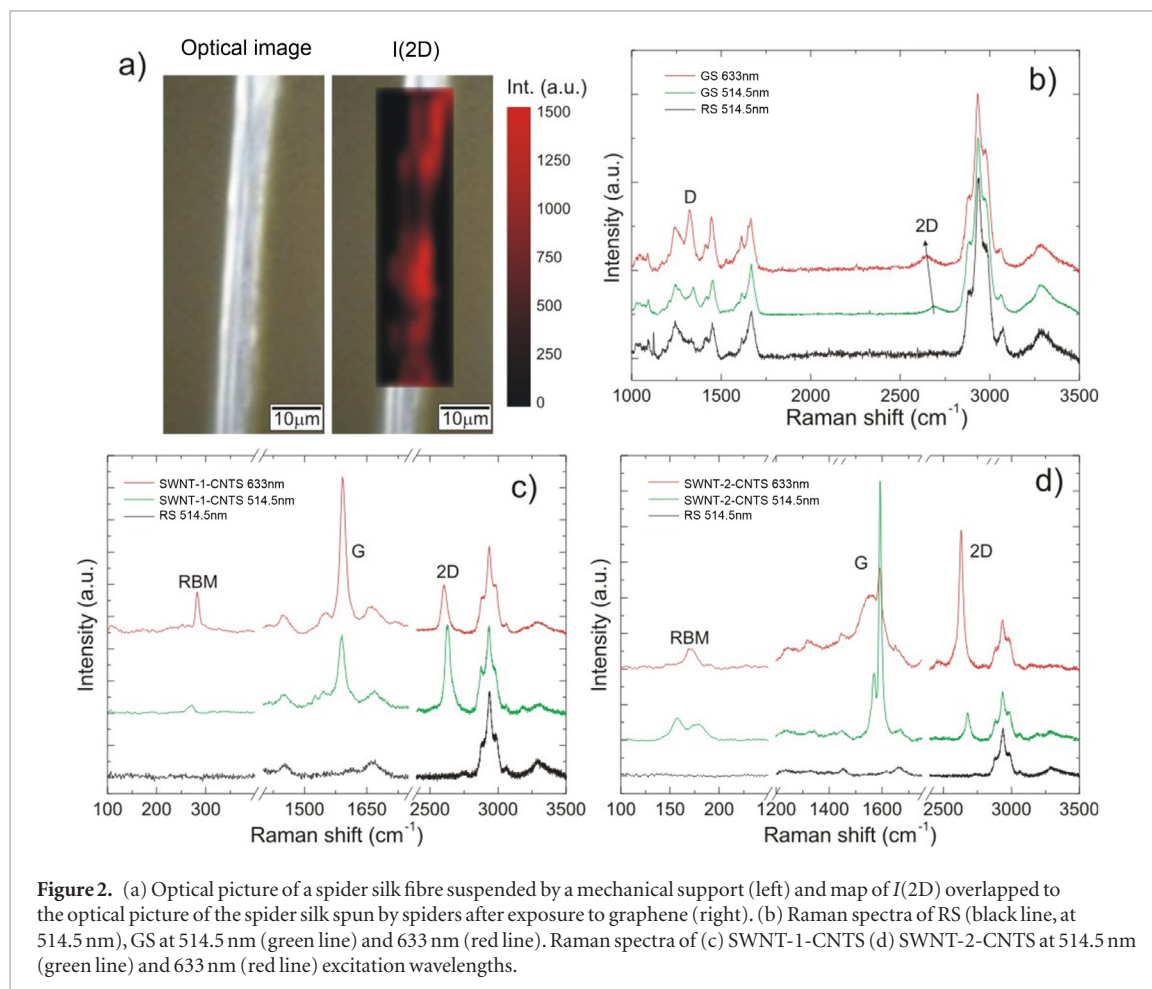
Successful attempts to improve the mechanical properties of spider silk have been limited [34, 40]. This is due to the difficulty of developing an adequate spinning methodology, balancing extrusion, drawing, yield and purity [41]. Naturally-spun fibres, obtained by forcible spinning [42], harvesting [43] or extracting spidroin (i.e. the main protein in dragline silk [2]) from glands [44], have reduced mechanical characteristics with respect to naturally-spun ones, e.g. due to the CO_2 anaesthesia of spiders

[45] and the consequent loss of active control of their silk spinning [46]. From a technological point of view, wet-spinning [47], electro-spinning [48], hand-drawing [42] or microfluidic approaches [49] have been investigated to produce an artificial silk at the laboratory scale, mechanically [34], structurally [40] or chemically [49] modified with respect to the natural one. However, a critical step is still needed to reach commercial-scale.

Here, we present a method for producing reinforced spider silk directly spun by spiders after their exposure to water dispersions of CNTs or graphene, as schematically shown in figure 1. This leads to improved mechanical properties, and a toughness modulus (defined as the area under the load-displacement curve, from the origin up to fracture [50, 51], per unit mass) surpassing synthetic polymeric high-performance fibres [52] and even the current toughest ‘knotted’ fibres [53–55].

Table 2. Mechanical properties (average values) of the first collection of silk samples produced after exposure of the spiders to CNTs or graphene (Spiders n. 1–6 with SWNT-1, spiders n. 7–10 with SWNT-2, spiders n. 11–15 with graphene). The largest increments in the silk mechanical properties are observed for spider 5 whereas the highest absolute values are observed for spider 7.

Spider n.	Diameter (μm)	Number of threads	Reinforcement	Young's modulus (GPa)	Ultimate strain (mm mm^{-1})	Fracture strength (MPa)	Toughness modulus (MPa)
1	0.57 ± 0.04	27	SWNT-1	3.9 ± 3.9	0.62 ± 0.65	326.1 ± 150.6	66.7 ± 60.9
2	0.43 ± 0.02	4	SWNT-1	40.1 ± 48.4	0.20 ± 0.16	3914.6 ± 5038.3	587.2 ± 820.3
3	0.77 ± 0.09	72	SWNT-1	8.7 ± 6.9	0.68 ± 0.37	1195.8 ± 1037.5	387.0 ± 384.7
4	0.76 ± 0.07	44	SWNT-1	2.4 ± 0.6	0.95 ± 0.52	579.4 ± 313.1	187.6 ± 66.7
5	0.78 ± 0.08	4	SWNT-1	37.9 ± 4.4	0.60 ± 0.28	3907.2 ± 874.1	1144.0 ± 555.3
6	0.84 ± 0.068	12	SWNT-1	9.6 ± 5.2	0.50 ± 0.24	954.3 ± 278.2	210.2 ± 87.3
7	1.00 ± 0.12	62	SWNT-2	47.8 ± 18.0	0.75 ± 0.09	5393.5 ± 1202.4	2143.6 ± 684.6
8	0.42 ± 0.08	34	SWNT-2	3.1 ± 1.1	0.41 ± 0.11	315.7 ± 124.7	47.8 ± 22.8
9	0.42 ± 0.04	82	SWNT-2	19.3 ± 6.3	0.34 ± 0.14	2034.9 ± 212.8	419.8 ± 96.2
10	0.81 ± 0.09	48	SWNT-2	0.2 ± 0.0	0.32 ± 0.02	20.1 ± 3.5	2.6 ± 1.8
11	0.67 ± 0.02	43	GS	0.8 ± 0.6	0.33 ± 0.19	58.0 ± 22.9	7.9 ± 3.4
12	0.74 ± 0.13	41	GS	4.9 ± 1.1	0.43 ± 0.06	607.5 ± 219.2	148.5 ± 71.6
13	0.66 ± 0.06	74	GS	3.1 ± 1.7	0.52 ± 0.37	421.8 ± 251.3	130.3 ± 129.0
14	1.02 ± 0.03	64	GS	0.4 ± 0.2	0.29 ± 0.08	45.9 ± 17.1	6.0 ± 2.8
15	0.61 ± 0.06	14	GS	13.0 ± 6.5	0.43 ± 0.24	1245.6 ± 559.4	254.7 ± 164.3



Results

Two types of CNTs are used in this study. The first is CoMoCAT [56] (~ 0.6 – 1.35 nm diameter) single-wall nanotubes (SWNT-1). The second is electric arc discharge SWNTs (P2) from Carbon solutions inc. (SWNT-2). CNT dispersions are prepared by adding

1 mg/10 ml weight-to-volume ratio of each CNT source to an aqueous solution of 2% w/v sodium deoxycholate (SDC, from Sigma-Aldrich Ltd) in deionised water. This surfactant is not harmful for the spiders, as discussed in the supplementary information (SI) (stacks.iop.org/TDM/4/031013/mmedia). De-bundling is obtained via ultrasonication using a Branson Ultrasonic Processor

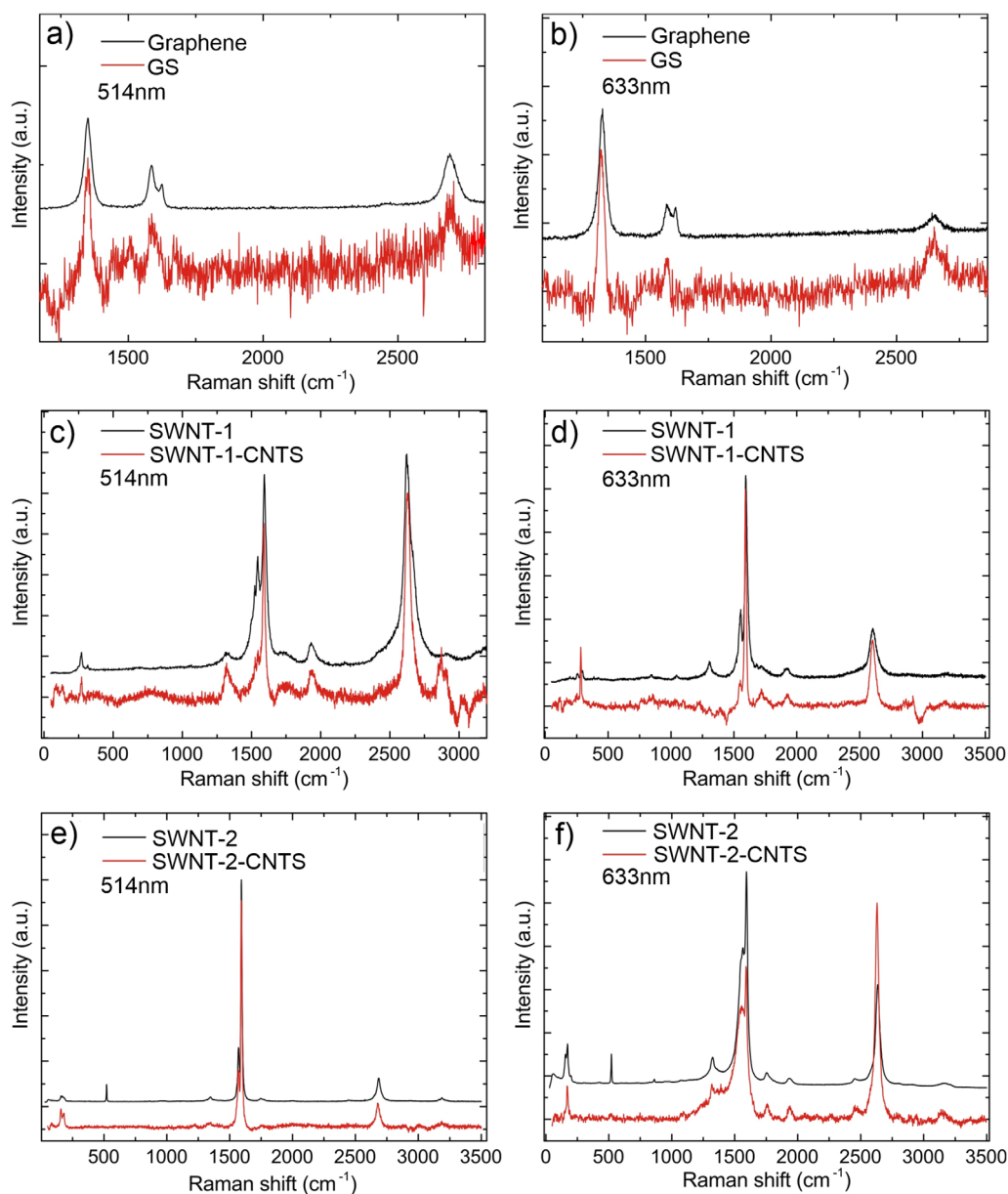
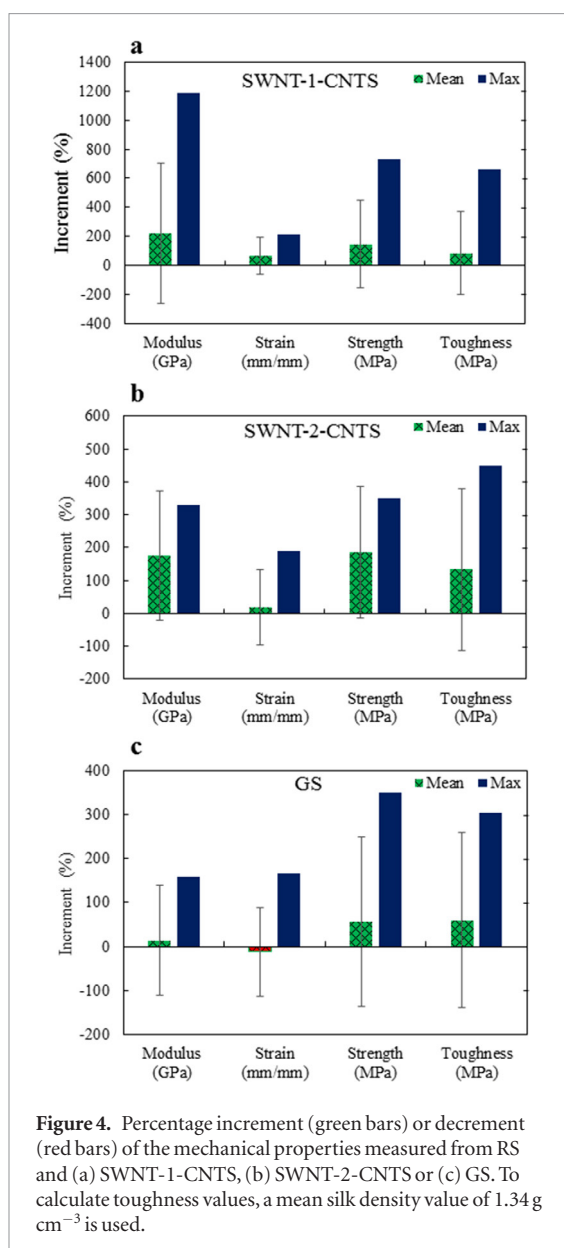


Figure 3. Raman spectra of graphene (black line) and GS (red line) at (a) 514.5 nm and (b) 633 nm. Raman spectra of SWNT-1, SWNT-2 and SWNT-1-CNTS and SWNT-2-CNTS at (c) and (e) 514.5 nm and (d) and (f) 633 nm excitation wavelengths.

for 2 h (450 kW at 20 kHz). The dispersions are ultracentrifuged using a TH-641 swinging bucket rotor in a Sorvall WX-100 at 200 000 g for 2 h at 18 °C to remove bundles and other impurities, such as amorphous carbon and catalyst residuals [57]. The supernatant of the two dispersions after ultracentrifugation is collected using pipettes and used for the characterization. Graphite flakes are sourced from Sigma Aldrich Ltd. 100 mg are dispersed in 10 ml water with 2% volume to weight (v/w) SDC. The dispersion is then ultrasonicated for 10 h and subsequently ultracentrifuged, exploiting sedimentation-based separation (SBS) [58] using a TH-641 swinging bucket rotor in a Sorvall WX-100 ultracentrifuge at 5000 rpm for 30 min. After ultracentrifugation, the supernatant is extracted by pipetting. The concentration of graphitic flakes is determined from the optical absorption coefficient at 660 nm [59]. A full optical and spectroscopic

characterization of the samples is presented in SI. This shows that the samples consist of ~60% single- (SLG) and ~40% few-layer (FLG) graphene flakes [60].

21 spiders of three species were selected (*Pholcidae Holocnemus*, *Pholcidae Pholcus* and *Theridiidae Steatoda*) as described in the SI. The spiders are exposed to the aqueous dispersions by spraying them in a corner of the box they are contained in, avoiding intentional direct spraying on the animals. The dragline silk is collected from 2 to 12 days later, in order to allow sufficient time for ingestion of the aqueous dispersions and the production of silk. 29% of the spiders died before the first silk collection, and a further 24% after 12 days, during which starvation could have come into play. The silk fibres consist of multiple threads of approximately circular cross-section. The average diameter of the single threads is determined for each sample through field emission



scanning electron microscopy (see SI), at two different cross-sections along their length. The number of threads in each fibre is also counted. The presence of CNTs and graphene is monitored by Raman spectroscopy.

Nano-tensile tests are performed under controlled conditions as described in the SI. Samples are prepared by fixing silk fibre ends to ‘C’ shaped cardboard holders (then cut after mounting in the sample holder, figure 1(b)), and subjected to traction up to failure in an Agilent T150 nanotensile system at a constant strain rate of $0.1\% \text{ s}^{-1}$, consistently with previous studies on spider silk mechanics [4, 61–63]. The stress σ , strain ε , and Young’s modulus E , are calculated as $\sigma = F/A_0$, $\varepsilon = \Delta l/l_0$, $E = d\sigma/d\varepsilon|_0$, where F is the force measured by the nanotensile system (see SI for details), A_0 is the cross-section area of the fibre, l_0 its initial length, and Δl the change in fibre length during the test. The area underlying the stress–strain curve corresponds to the energy per unit volume required to break the fibre,

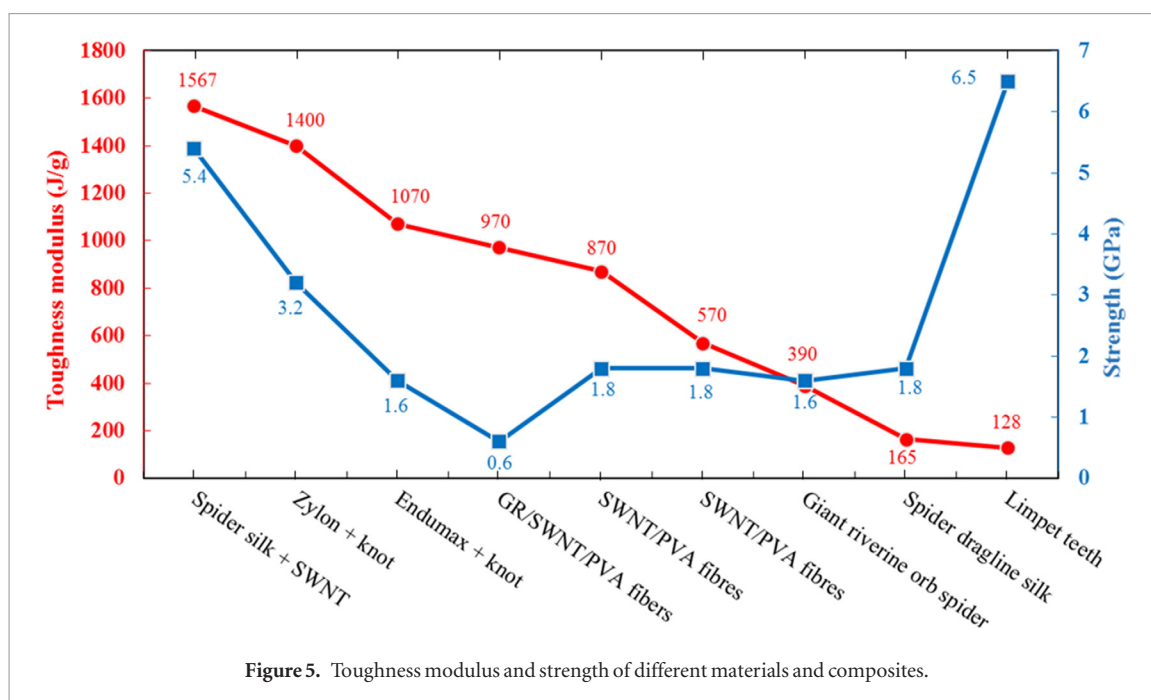
the so-called toughness modulus T , also alternatively given in energy per unit mass, as derived by dividing the energy per unit volume by the density of the material: $T = \frac{1}{\rho} \int \sigma d\varepsilon$ [53].

The diameter of the cross-sectional area of the silk fibres is between ~ 5 and $\sim 10 \mu\text{m}$, as obtained by multiplying the mean value of the measured cross-sectional area of the threads by their total number. The resulting diameters and number of threads for each fibre are reported in tables 1 and 2 for the reference spider silk (RS) and that collected from spiders exposed to dispersions of graphene (GS) and SWNTs (CNTS).

Figure 2 shows an optical image of a suspended fibre (figure 2(a)) and compares the Raman spectra of RS with that of GS (figure 2(b)) and CNTS (figures 2(c) and (d)). The RS Raman spectrum comprises several peaks in the $1000\text{--}1800 \text{ cm}^{-1}$ and $2700\text{--}3500 \text{ cm}^{-1}$ regions. The peaks at ~ 1088 and 1160 cm^{-1} are characteristic of the $n(\text{C}\text{--}\text{C})$ skeletal band of polypeptide chains [64, 65]. Two intense bands are also seen at $\sim 1230 \text{ cm}^{-1}$, characteristic of amide III groups in π -sheets structured proteins [66, 67] and at $\sim 1444 \text{ cm}^{-1}$ assigned to CH_2 bending modes, both bands typically found in the Raman spectrum of spider silk [68]. The peaks at 1615 cm^{-1} and 1665 cm^{-1} are assigned to $n(\text{CO})$ amide I bands characteristic of the π -sheets configuration for the polypeptide backbone [66, 68]. The Raman peaks in the region $2700\text{--}3500 \text{ cm}^{-1}$ are typical of C–H and N–H vibrations [67].

Raman spectra from GS and CNTS samples are shown in figure 3. The spectra are normalized with respect to the C–H band at $\sim 2934 \text{ cm}^{-1}$, the most intense in RS. The normalized RS spectrum is then subtracted from the GS and CNTS ones. Figures 3(a) and (b) show that the spectrum of the flakes in the dispersion is compatible with that of GS. At both 514 and 633 nm, the D to G and 2D to G intensity ratios, $I(\text{D})/I(\text{G})$ and $I(2\text{D})/I(\text{G})$, as well as the positions of the G and 2D peaks, $\text{Pos}(\text{G})$ and $\text{Pos}(2\text{D})$, are very similar. The comparison indicates that graphene detected in GS has a similar level of disorder [69–72] as the original material. The same holds for CNTS. Figures 2(c)–(f) show that the spectra of the original SWNTs and those measured on CNTS are similar, indicating a negligible change in the structural properties.

A summary of the mechanical properties of RS, GS and CNTS is reported in tables 1 and 2, and typical stress–strain curves of the silk fibres are presented in figure 1(c) and in the SI. Scatter in the data is large, mainly due to the variability in the properties of the collected silk samples, deriving from spiders of different species and ages (see SI), but also from factors such as the sensitivity of silk density to humidity [73]. However, fibre slippage in the loading frame can be excluded, since this would be noticeable in the stress–strain curves, given the high-sensitivity (50 nN load resolution and 0.1 nm displacement resolution) of



the nanotensile testing system. Ultimate strain values have smaller scatter, since they are not dependent on parameters such as fibre cross-sectional area. In CNTs and GS, the scatter is greater due to the varying CNTs and flakes concentrations, since there is no control on the nanoparticle uptake mechanism at this stage. Apart from this, there is an intrinsic variability of mechanical properties of different samples of the same silk, in line with previous studies [62, 74–76].

To avoid these problems, we focus on the variation in mechanical properties of the silk fibres from individual spider specimens before and after exposure. The average and maximum variations are shown in figure 4. Fracture strength, Young's modulus and toughness increase on average between 80 and 220% in CNTs and between 15% and 60% for GS. The highest fracture strength and Young's modulus increments are +731% (3.9 GPa) and +1183% (37.9 GPa) for CNTs, with an increment \sim +663% in toughness (2.1 GPa). This corresponds to 1567 J g^{-1} , calculated using an average silk density value $\sim 1.34 \text{ g cm}^{-3}$ [53], neglecting changes due to humidity or the presence of CNTs or graphene, as discussed in the SI, with a 41% decrement of ultimate strain (0.6 mm mm^{-1}). This should be compared to the toughest silk fibres found to date, having a toughness $\sim 520 \text{ MJ m}^{-3}$ [62], and a strength $\sim 1.65 \text{ GPa}$ [62]. The combination of increment in toughness and decrement in ultimate strain is peculiar and fundamental in applications such as parachutes or bullet-proof vests, where high performance textiles are required to stop bullets in millimetres [77]. The second highest increments \sim +350% (2.0 GPa) in fracture strength and +330% (19.3 GPa) in Young's modulus are found for SWNT-2-CNTs, corresponding to an increment \sim +204% in toughness (0.4 GPa), with a decrement \sim 36% in ultimate strain (0.3 mm mm^{-1}). A smaller, but still significant, increment is also observed for some of the fibres containing GS, with +151% (1.2 GPa) in fracture

strength and +142% (13.0 GPa) in Young's modulus, corresponding to an increment of both toughness and ultimate strain of +250% (0.3 GPa) and +166% (0.4 mm mm^{-1}), respectively.

We note that Wang *et al* [78] reported a similar approach to that described here, based on the initial posting of the present manuscript [79], cited as reference [19] in [78] and applied it to silkworm silk. This demonstrates that our approach is reproducible in other biological systems. However, Wang *et al* [78] achieved far inferior mechanical properties to those reported here. Indeed, in the best case we get here a strength $\sim 5.4 \text{ GPa}$ and toughness modulus $\sim 1567 \text{ J g}^{-1}$, whilst Wang *et al* [78] achieves maximum values $\sim 0.6 \text{ GPa}$ and $\sim 400 \text{ J g}^{-1}$, respectively. This is mainly due to lower mechanical properties of silkworm silk with respect to spider silk [1–4].

Discussion

Figure 5 compares the strength and toughness of various natural and artificial materials. The best fibre obtained in this study displays higher strength than high-performance polymeric fibres like Zylon or Endumax [52, 53], or SWNT/carbon-reinforced polymeric fibres [80–82], and is surpassed only by T1000[®] Carbon fibres [83] or goethite nanofibres found in limpet teeth [27]. At the same time, its toughness is significantly higher than the toughest spider silks found in nature [62, 75] or high-toughness SWNT/PVA fibres [80]. Indeed, it exceeds the previous largest recorded toughness value for synthetic polymer fibres or CNT microfibrils with integrated knots as energy dissipators [54].

Molecular Dynamics simulations reported in the SI show that CNTs have the strongest interaction with the mannose-associated serine protease 1 (MASP1) spider silk fibers, in the amorphous region where

they affect the structure of the bundle. The measured strength and stiffness data can be compared to analytical predictions for the reinforcing effect of graphene or CNTs on silk using the direct and inverse rule of mixtures [84] and simulations using the Hierarchical Fibre Bundle Model [85] (see SI). These can estimate the concentration of reinforcements by fitting the corresponding experimental strength values, giving equivalent volume fractions in GS and CNTS between 1% (spider 15) and 15% (spider 7), with an average ~7%.

Graphene flakes appear to be a less effective reinforcement than CNTs (figure 4(c)). This could be due to the shape of the flakes. The lateral characteristic dimensions of our flakes (~200–300 nm), two orders of magnitude larger than the characteristic CNT diameter, could give rise to less efficient load transfer, since their longitudinal dimension could be smaller than the critical length (of the order of microns and dependent on the interface properties) predicted by the shear lag theory for optimal load transfer [86]. Inefficient load transfer could also be due to the crumpled configuration of the flakes or a larger misalignment with respect to CNTs. Finding solutions for these problems could potentially enable GS with mechanical properties superior to CNTS, thanks to the two surfaces available for load transfer in flakes [86]. Tuning the constitutive law of the silk could also maximize the robustness of an entire structure [87].

Conclusions

Spiders placed in an environment with water solutions containing nanotubes or graphene may produce dragline silk with enhanced mechanical properties, realizing the highest fibre toughness to date, combined with a strength comparable to that of the strongest carbon fibres or of limpet teeth. Our proof-of-concept experiment paves the way to exploiting the naturally efficient spider spinning process to produce reinforced silk fibres, thus further improving one of the most promising silk materials, as compared to synthetic recombinant silks. This procedure of natural integration of reinforcements in biological structural materials could also be applied to other animals and plants, leading to a new class of ‘bionicomposites’ for innovative applications.

Acknowledgments

We thank V Morandi and R Mazzaro for the transmission electron microscopy images in the SI. We acknowledge ‘Nanofacility Piemonte’ at the INRIM Institute for the FESEM, a Newton International Fellowship, EPSRC grants EP/K01711X/1, EP/K017144/1, ERC grant SILKENE, Hetero2D, HiGRAPHINK, FET Proactive NEUROFIBRES and the EU Graphene Flagship. This paper is dedicated to the memory of Prof. Franco Montevicchi.

ORCID iDs

Federico Bosia  <https://orcid.org/0000-0002-2886-4519>

Francesco Bonaccorso  <https://orcid.org/0000-0001-7238-9420>

Simone Taioli  <https://orcid.org/0000-0003-4010-8000>

Giovanni Garberoglio  <https://orcid.org/0000-0002-9201-2716>

Nicola M Pugno  <https://orcid.org/0000-0003-2136-2396>

References

- [1] Shao Z Z and Vollrath F 2002 Materials: Surprising strength of silkworm silk *Nature* **418** 741
- [2] Atkins E 2003 Silk’s secrets *Nature* **424** 1010
- [3] Agnarsson I, Boutry C and Blackledge T A 2008 Spider silk aging: initial improvement in a high performance material followed by slow degradation *J. Exp. Zool. A* **309** 494–504
- [4] Swanson B O, Blackledge T A, Beltran J and Hayashi C Y 2006 Variation in the material properties of spider dragline silk across species *Appl. Phys. A* **82** 213–8
- [5] Vollrath F, Porter D and Holland C 2013 The science of silks *MRS Bull.* **38** 73–80
- [6] Huang X P, Liu G Q and Wang X W 2012 New secrets of spider silk: exceptionally high thermal conductivity and its abnormal change under stretching *Adv. Mater.* **24** 1482–6
- [7] Foelix R F 2011 *Biology of Spiders* (Oxford: Oxford University Press)
- [8] Eisoldt L, Smith A and Scheibel T 2011 Decoding the secrets of spider silk *Mater Today* **14** 80–6
- [9] Byrom D 1991 *Biomaterials: Novel Materials from Biological Sources* (Palgrave Macmillan)
- [10] Laible R 2012 *Ballistic Materials and Penetration Mechanics* (Amsterdam: Elsevier)
- [11] Kubik S 2002 High-performance fibers from spider silk *Angew. Chem. Int. Ed.* **41** 2721
- [12] Scott A 2014 Spider silk poised for commercial entry *Chem. Eng. News* **92** 24–7
- [13] Harvey D, Bardelang P, Goodacre S L, Cockayne A and Thomas N R 2017 Antibiotic spider silk: site-specific functionalization of recombinant spider silk using ‘click’ chemistry *Adv. Mater.* **29**
- [14] Kuhbier J W, Reimers K, Kasper C, Allmeling C, Hillmer A, Menger B, Vogt P M and Radtke C 2011 First investigation of spider silk as a braided microsurgical suture *J. Biomed. Mater. Res. B* **97B** 381–7
- [15] Allmeling C, Jokuszies A, Reimers K, Kall S, Choi C Y, Brandes G, Kasper C, Scheper T, Guggenheim M and Vogt P M 2008 Spider silk fibres in artificial nerve constructs promote peripheral nerve regeneration *Cell Prolif.* **41** 408–20
- [16] Marelli B, Brenckle M A, Kaplan D L and Omenetto F G 2016 Silk fibroin as edible coating for perishable food preservation *Sci. Rep.* **6** 25263
- [17] Babu K M 2013 *Silk: Processing, Properties and Applications* (Oxford: Woodhead Publishing)
- [18] Hennecke K, Redeker J, Kuhbier J W, Strauss S, Allmeling C, Kasper C, Reimers K and Vogt P M 2013 Bundles of spider silk, braided into sutures, resist basic cyclic tests: potential use for flexor tendon repair *Plos One* **8** e61100
- [19] Keten S and Buehler M J 2010 Nanostructure and molecular mechanics of spider dragline silk protein assemblies *J. R. Soc. Interface* **7** 1709–21
- [20] Silva L P and Rech E L 2013 Unravelling the biodiversity of nanoscale signatures of spider silk fibres *Nat. Commun.* **4** 3014

- [21] Porter D and Vollrath F 2009 Silk as a biomimetic ideal for structural polymers *Adv. Mater.* **21** 487–92
- [22] Heim M, Keerl D and Scheibel T 2009 Spider silk: from soluble protein to extraordinary fiber *Angew. Chem. Int. Ed.* **48** 3584–96
- [23] Vollrath F, Madsen B and Shao Z Z 2001 The effect of spinning conditions on the mechanics of a spider's dragline silk *Proc. R. Soc. B* **268** 2339–46
- [24] George A and Ravindran S 2010 Protein templates in hard tissue engineering *Nano Today* **5** 254–66
- [25] Lichtenegger H C, Schoberl T, Bartl M H, Waite H and Stucky G D 2002 High abrasion resistance with sparse mineralization: copper biomineral in worm jaws *Science* **298** 389–92
- [26] Politi Y, Metzler R A, Abrecht M, Gilbert B, Wilt F H, Sagi I, Addadi L, Weiner S and Gilbert P U P A 2008 Transformation mechanism of amorphous calcium carbonate into calcite in the sea urchin larval spicule *Proc. Natl Acad. Sci.* **105** 17362–6
- [27] Barber A H, Lu D and Pugno N M 2015 Extreme strength observed in limpet teeth *J. R. Soc. Interface* **12** 20141326
- [28] Broomell C C, Zok F W and Waite J H 2008 Role of transition metals in sclerotization of biological tissue *Acta Biomater.* **4** 2045–51
- [29] Broomell C C, Mattoni M A, Zok F W and Waite J H 2006 Critical role of zinc in hardening of Nereis jaws *J. Exp. Biol.* **209** 3219–25
- [30] Cribb B W, Stewart A, Huang H, Truss R, Noller B, Rasch R and Zalucki M P 2007 Insect mandibles-comparative mechanical properties and links with metal incorporation *Naturwissenschaften* **95** 17–23
- [31] Edwards A J, Fawke J D, McClements J G, Smith S A and Wyeth P 1993 Correlation of zinc distribution and enhanced hardness in the mandibular cuticle of the leaf-cutting ant *Atta sexdens rubropilosa* *Cell Biol. Int.* **17** 697–8
- [32] Mayes E L, Vollrath F and Mann S 1998 Fabrication of magnetic spider silk and other silk-fiber composites using inorganic nanoparticles *Adv. Mater.* **10** 801–5
- [33] Chu M Q and Sun Y 2007 Self-assembly method for the preparation of near-infrared fluorescent spider silk coated with CdTe nanocrystals *Smart Mater. Struct.* **16** 2453–6
- [34] Steven E, Saleh W R, Lebedev V, Acquah S F A, Laukhin V, Alamo R G and Brooks J S 2013 Carbon nanotubes on a spider silk scaffold *Nat. Commun.* **4** 2435
- [35] Lee S-M, Pippel E, Gösele U, Dresbach C, Qin Y, Chandran C V, Bräuniger T, Hause G and Knez M 2009 Greatly increased toughness of infiltrated spider silk *Science* **324** 488–92
- [36] Allmeling C, Jokuszies A, Reimers K, Kall S and Vogt P M 2006 Use of spider silk fibres as an innovative material in a biocompatible artificial nerve conduit *J. Cell. Mol. Med.* **10** 770–7
- [37] Dal Pra I, Chiarini A, Boschi A, Freddi G and Armato U 2006 Novel dermo-epidermal equivalents on silk fibroin-based formic acid-crosslinked three-dimensional nonwoven devices with prospective applications in human tissue engineering/regeneration/repair *Int. J. Mol. Med.* **18** 241–7
- [38] Agnarsson I, Dhinojwala A, Sahni V and Blackledge T A 2009 Spider silk as a novel high performance biomimetic muscle driven by humidity *J. Exp. Biol.* **212** 1989–93
- [39] Dal Pra I, Freddi G, Minic J, Chiarini A and Armato U 2005 De novo engineering of reticular connective tissue *in vivo* by silk fibroin nonwoven materials *Biomaterials* **26** 1987–99
- [40] Brown C P, Rosei F, Traversa E and Licoccia S 2011 Spider silk as a load bearing biomaterial: tailoring mechanical properties via structural modifications *Nanoscale* **3** 870–6
- [41] Hardy J G, Romer L M and Scheibel T R 2008 Polymeric materials based on silk proteins *Polymer* **49** 4309–27
- [42] Pérez-Rigueiro J, Elices M, Plaza G, Real J I and Guinea G V 2005 The effect of spinning forces on spider silk properties *J. Exp. Biol.* **208** 2633–9
- [43] Lewis R 1996 Unraveling the weave of spider silk: One of nature's wondrous chemical structures is being dissected so that it can be used in human inventions *BioScience* **46** 636–8
- [44] Kenney J M, Knight D, Wise M J and Vollrath F 2002 Amyloidogenic nature of spider silk *Eur. J. Biochem.* **269** 4159–63
- [45] Guinea G V, Elices M, Real J I, Gutierrez S and Perez-Rigueiro J 2005 Reproducibility of the tensile properties of spider (*Argiope trifasciata*) silk obtained by forced silking *J. Exp. Zool. A* **303A** 37–44
- [46] Blackledge T A, Swindeman J E and Hayashi C Y 2005 Quasistatic and continuous dynamic characterization of the mechanical properties of silk from the cobweb of the black widow spider *Latrodectus hesperus* *J. Exp. Biol.* **208** 1937–49
- [47] Liu Y, Shao Z and Vollrath F 2005 Extended wet-spinning can modify spider silk properties *Chem. Commun.* 2489–91
- [48] Oh H J, Pant H R, Kang Y S, Jeon K S, Pant B, Kim C S and Kim H Y 2012 Synthesis and characterization of spider-web-like electrospun mats of meta-aramid *Polym. Int.* **61** 1675–82
- [49] Peng Q, Zhang Y, Lu L, Shao H, Qin K, Hu X and Xia X 2016 Recombinant spider silk from aqueous solutions via a bio-inspired microfluidic chip *Sci. Rep.* **6** 36473
- [50] De Silva C W 2014 *Mechanics of Materials* (Boca Raton, FL: CRC Press)
- [51] Rao D S 2002 *Introduction to Strength of Materials* (Universities Press)
- [52] Bhat G 2017 *Structure and Properties of High-Performance Fibers* (Oxford: Woodhead Publishing)
- [53] Pugno N M 2014 The 'egg of columbus' for making the world's toughest fibres *Plos One* **9** e93079
- [54] Bosia F, Lepore E, Alvarez N T, Miller P, Shanov V and Pugno N M 2016 Knotted synthetic polymer or carbon nanotube microfibrils with enhanced toughness, up to 1400 J g⁻¹ *Carbon* **102** 116–25
- [55] Pantano M F, Berardo A and Pugno N M 2016 Tightening slip knots in raw and degummed silk to increase toughness without losing strength *Sci. Rep.* **6** 18222
- [56] www.sigmaaldrich.com/materials-science/nanomaterials/comocat-carbon-nanotubes.html
- [57] Bonaccorso F, Hasan T, Tan P H, Sciascia C, Privitera G, Di Marco G, Gucciardi P G and Ferrari A C 2010 Density gradient ultracentrifugation of nanotubes: interplay of bundling and surfactants encapsulation *J. Phys. Chem. C* **114** 17267–85
- [58] Bonaccorso F, Lombardo A, Hasan T, Sun Z, Colombo L and Ferrari A C 2012 Production and processing of graphene and 2d crystals *Mater. Today* **15** 564–89
- [59] Torrisi F *et al* 2012 Inkjet-printed graphene electronics *ACS Nano* **6** 2992–3006
- [60] Marago O M *et al* 2010 Brownian motion of graphene *ACS Nano* **4** 7515–23
- [61] Lepore E, Marchioro A, Isaia M, Buehler M J and Pugno N M 2012 Evidence of the most stretchable egg sac silk stalk, of the European spider of the year meta menardi *Plos One* **7** e30500
- [62] Agnarsson I, Kuntner M and Blackledge T A 2010 Bioprospecting finds the toughest biological material: extraordinary silk from a giant riverine orb spider *Plos One* **5** e11234
- [63] Sahni V, Blackledge T A and Dhinojwala A 2010 Viscoelastic solids explain spider web stickiness *Nat. Commun.* **1** 19
- [64] Colomban P, Dinh H M, Riand J, Prinsloo L C and Mauchamp B 2008 Nanomechanics of single silkworm and spider fibres: a Raman and micro-mechanical *in situ* study of the conformation change with stress *J. Raman Spectrosc.* **39** 1749–64
- [65] Edwards H G M and Farwell D W 1995 Raman-spectroscopic studies of silk *J. Raman Spectrosc.* **26** 901–9
- [66] Williams A C, Barry B W and Edwards H G M 1994 Comparison of Fourier-transform Raman-spectra of mammalian and reptilian skin *Analyst* **119** 563–6
- [67] Socrates G 2004 *Infrared and Raman Characteristic Group Frequencies: Tables and Charts* 3rd edn (New York: Wiley)
- [68] Shao Z, Vollrath F, Sirichaisit J and Young R J 1999 Analysis of spider silk in native and supercontracted states using Raman spectroscopy *Polymer* **40** 2493–500
- [69] Ferrari A C and Basko D M 2013 Raman spectroscopy as a versatile tool for studying the properties of graphene *Nat Nano* **8** 235–46
- [70] Bruna M, Ott A K, Ijäs M, Yoon D, Sassi U and Ferrari A C 2014 Doping dependence of the Raman spectrum of defected graphene *ACS Nano* **8** 7432–41

- [71] Cançado L G, Jorio A, Ferreira E H M, Stavale F, Achete C A, Capaz R B, Moutinho M V O, Lombardo A, Kulmala T S and Ferrari A C 2011 Quantifying defects in graphene via Raman spectroscopy at different excitation energies *Nano Lett.* **11** 3190–6
- [72] Ferrari A C and Robertson J 2000 Interpretation of Raman spectra of disordered and amorphous carbon *Phys. Rev. B* **61** 14095–107
- [73] Vehoff T, Glisovic A, Schollmeyer H, Zippelius A and Salditt T 2007 Mechanical properties of spider dragline silk: humidity, hysteresis, and relaxation *Biophys. J.* **93** 4425–32
- [74] Moore A M F and Tran K 1999 Material properties of cobweb silk from the black widow spider *Latrodectus hesperus* *Int. J. Biol. Macromol.* **24** 277–82
- [75] Swanson B O, Blackledge T A, Summers A P and Hayashi C Y 2006 Spider dragline silk: correlated and mosaic evolution in high-performance biological materials *Evolution* **60** 2539–51
- [76] Blackledge T A and Hayashi C Y 2006 Silken toolkits: biomechanics of silk fibers spun by the orb web spider *Argiope argentata* (Fabricius 1775) *J. Exp. Biol.* **209** 2452–61
- [77] Peleg K, Rivkind A and Aharonson-Daniel L 2006 Does body armor protect from firearm injuries? *J. Am. Coll. Surg.* **202** 643–8
- [78] Wang Q, Wang C Y, Zhang M C, Jian M Q and Zhang Y Y 2016 Feeding single-walled carbon nanotubes or graphene to silkworms for reinforced silk fibers *Nano Lett.* **16** 6695–700
- [79] Lepore E, Bonaccorso F, Bruna M, Bosia F, Taioli S, Garberoglio G, Ferrari A C and Pugno N M 2015 Silk reinforced with graphene or carbon nanotubes spun by spiders arXiv:1504.06751
- [80] Miaudet P, Badaire S, Maugey M, Derré A, Pichot V, Launois P, Poulin P and Zakri C 2005 Hot-drawing of single and multiwall carbon nanotube fibers for high toughness and alignment *Nano Lett.* **5** 2212–5
- [81] Dalton A B, Collins S, Munoz E, Razal J M, Ebron V H, Ferraris J P, Coleman J N, Kim B G and Baughman R H 2003 Super-tough carbon-nanotube fibres *Nature* **423** 703
- [82] Vilatela J J and Windle A H 2010 Yarn-like carbon nanotube fibers *Adv. Mater.* **22** 4959
- [83] Liu J, Yue Z and Fong H 2009 Continuous nanoscale carbon fibers with superior mechanical strength *Small* **5** 536–42
- [84] Askeland D R, Fulay P P and Wright W J 2011 *The Science and Engineering of Materials* (Stamford, CT: Cengage Learning)
- [85] Pugno N M, Bosia F and Abdalrahman T 2012 Hierarchical fiber bundle model to investigate the complex architectures of biological materials *Phys. Rev. E* **85** 011903
- [86] Pugno N M 2013 Towards the Artsutanov's dream of the space elevator: the ultimate design of a 35 GPa strong tether thanks to graphene *Acta Astronaut.* **82** 221–4
- [87] Cranford S W, Tarakanova A, Pugno N M and Buehler M J 2012 Nonlinear material behaviour of spider silk yields robust webs *Nature* **482** 72–6